Neural Computing and Applications (2024) 36:2737–2748
https://doi.org/10.1007/s00521-023-09125-4

ORIGINAL ARTICLE

Adaptive prescribed performance control for state constrained stochastic nonlinear systems with unknown control direction: a novel network-based approach

Yu-Qun Han[1,2] · Na Li[1] · Dong-Mei Wang[1] · Ya-Feng Zhou[1] · Shan-Liang Zhu[1,2]

Received: 24 October 2022 / Accepted: 16 October 2023 / Published online: 23 November 2023

Abstract
In this paper, the tracking control problem of the state constrained stochastic nonlinear systems with unknown control direction is studied, and a novel adaptive prescribed performance control (PPC) approach is developed with the help of the multi-dimensional Taylor network (MTN). Firstly, a performance function is introduced into the first step of backstepping to ensure transient performance under state constraints. Secondly, the tangent time-varying barrier Lyapunov functions (tan-TVBLFs) are constructed to prevent all states from violating the given time-varying boundary. Thirdly, the MTNs are employed to estimate the unknown nonlinearity in the process of controller design, and a new adaptive PPC strategy is designed. Then, the Lyapunov stability theorem is used to prove that the closed-loop system is semi-global uniformly ultimately bounded (SGUUB) in probability, and the tracking error can be kept in an adjustable small neighborhood of the origin. Finally, the effectiveness of the proposed scheme is verified by the simulation of a numerical example and an actual control system.

Keywords Stochastic nonlinear systems · State constrained · Adaptive tracking control · Prescribed performance · Multi-dimensional Taylor network

1 Introduction

It is well-known that the existence of stochastic phenomena often leads to the deterioration of the controlled systems, which can cause great difficulties in the controller design and stability study of the systems. Therefore, the study of control theory of stochastic nonlinear systems plays a key role in practical scientific and technological applications, which has attracted widespread attention [1–3]. With decades of development, many methods for solving nonlinear systems have been extended to stochastic nonlinear systems, and many meaningful results have been achieved [4–7]. In particular, it is worth noting that the adaptive backstepping control has become a popular control method for nonlinear systems due to its applicability to uncertain systems, which has also made significant progress in stochastic nonlinear systems [8–11]. However, the parameter uncertainty that exists in the controlled systems may make the traditional adaptive backstepping scheme unapplicable. This drawback makes it difficult to carry out the above results in practical engineering.

Driven by the above problem, many intelligent control methods, such as neural networks (NNs)-based control and fuzzy logic systems (FLSs)-based control, have been proposed [12–15]. In particular, combining the adaptive backstepping technique with the above intelligent control methods can lead to more effective results [16–19]. Recently, multi-dimensional Taylor network (MTN), a new neural network (NN) with special structure, provided a new approximation method for complex nonlinear systems. In view of MTN has the advantages of improving the convergence speed and reducing the computational complexity, the MTN-based approach has been successfully applied to general nonlinear systems [20], single-input single-

Yu-Qun Han and Na Li have contributed equally to this work.

✉ Shan-Liang Zhu
zhushanliang@qust.edu.cn

[1] School of Mathematics and Physics, Qingdao University of Science and Technology, Qingdao 266061, China

[2] Research Institute for Mathematics and Interdisciplinary Sciences, Qingdao University of Science and Technology, Qingdao 266061, China

output (SISO) nonlinear systems [21, 22], multiple-input multiple-output (MIMO) nonlinear systems [23, 24], and stochastic nonlinear systems [25–27]. Although the MTN-based approach has obtained plentiful and substantial achievements in the control field, most of the results focused on nonlinear systems without state constrained. More recently, a growing attention has been devoted to state constrained stochastic nonlinear systems due to its important practical significance.

On the one hand, in practical engineering systems, the inputs and states of systems are frequently constrained by factors like input saturation [28], time delay [29, 30], and full state constraints [31, 32]. The safety of personnel and equipment can only be ensured by limiting the input or state to the allowed conditions. It is of interest to note that the system stability and satisfactory control performance can be achieved by limiting all states of the system to a given boundary. Thus, the full state constraints has become a popular research topic and has made notable achievements in stochastic nonlinear systems [31–33]. Meanwhile, the adaptive MTN-based control has also been applied to stochastic nonlinear systems with full state constraints [34, 35]. On the other hand, prescribed performance control (PPC) has obtained growing attention since this control approach can improve the transient and stability performance of the controlled systems. The underlying idea of PPC is to limit the output of the controlled systems to the envelope, which can make sure that the convergence speed and overshoot meet the prescribed requirements. Based on the idea of PPC, a series of research results have been achieved for nonstrict-feedback stochastic nonlinear systems [36], MIMO stochastic nonlinear systems [37, 38], and large-scale nonlinear time delay systems [39]. Recently, the authors in [40] addressed the issue of stochastic nonlinear systems with full state constraints and proposed a new adaptive PPC strategy. However, to the best of the authors' knowledge, few studies have attempted to analyze the state constrained stochastic nonlinear systems with unknown control direction under PPC.

Based on the above research and discussion, this study tries to develop a novel MTN-based adaptive control strategy with prescribed performance for a class of stochastic nonlinear systems subject to unknown control direction and full state constraints. Compared with the existing literatures, the innovations of this work are as follows:

(1) To solve the time-varying full state constraints, the tangent time-varying barrier Lyapunov functions (tan-TVBLFs) are constructed in this paper, which can handle both constant and time-varying constraints. Although the authors in [32, 33] also addressed the problem of the full state constraints of stochastic nonlinear systems, they only focused on constant constraints rather than time-varying constraints.

(2) Compared with the existing literature on the PPC for nonlinear systems with partial and full state constraints [44], this paper proposes the MTN-based adaptive PPC strategy for state constrained stochastic nonlinear systems with unknown control direction. Although the authors in [36, 41–43] studied the PPC for stochastic nonlinear systems, the time-varying full state constraints were not considered. Therefore, the problem addressed in this paper is more general.

(3) In addition, even though the time-varying full state constraints was implemented in the stochastic nonlinear systems [31, 45], the PPC was unrealized. Similar to [31], this research prevents system states from violating constraints by constructing tan-TVBLFs. The interesting aspect is that this study builds a controller by employing MTN as an approximator, achieving the aim of reducing computational complexity while taking PPC into account. Compared with [46], the control scheme proposed in this paper can not only achieve full state constraints, but also implement the steady-state and transient performance of the system.

2 Problem formulation and preliminaries

2.1 System description

Consider the following stochastic nonlinear system

$$\begin{cases} dx_i = (f_i(\bar{\boldsymbol{x}}_i) + g_i(\bar{\boldsymbol{x}}_i)x_{i+1})dt + \phi_i^{\mathrm{T}}(\bar{\boldsymbol{x}}_i)d\omega \\ \quad i = 1, \ldots, n-1 \\ dx_n = (f_n(\bar{\boldsymbol{x}}_n) + g_n(\bar{\boldsymbol{x}}_n)u)dt + \phi_n^{\mathrm{T}}(\bar{\boldsymbol{x}}_n)d\omega \\ \quad y = x_1 \end{cases} \tag{1}$$

where $\bar{\boldsymbol{x}}_i = [x_1, x_2, \ldots, x_i]^{\mathrm{T}} \in R^i (i = 1, \ldots, n)$ stands the state vector of the system. $u \in R$ and $y \in R$ are the input and the output of the system, respectively. ω represents the r-dimensional standard Wiener process. $f_i(\bar{\boldsymbol{x}}_i)$ and $\phi_i(\bar{\boldsymbol{x}}_i)$ are the unknown smooth nonlinear functions with $f_i(\boldsymbol{0}) = 0$ and $\phi_i(\boldsymbol{0}) = 0$. $g_i(\bar{\boldsymbol{x}}_i)$ denote the unknown smooth nonlinear functions, which represent the unknown control direction of the system. In particular, all state variables of the system (1) satisfy the constraint boundary $\Omega_{x_i} = \{x_i \in R \,|\, |x_i| < k_{c,i}(t), i = 1 \ldots n\}$ and $k_{c,i}(t)$ is a function of time t.

For a given reference signal y_d, the control objectives of this paper are to design an adaptive controller for system

(1) such that: (a) all signals in the closed-loop systems are SGUUB in probability; (b) all states variables are bounded and never violate the given constraint boundary; (c) the system output y can effectively track the reference signal y_d and the tracking error is constrained within the prescribed performance boundary.

The following Assumptions are needed to facilitate controller design.

Assumption 1 [14] Supposing the unknown smooth nonlinear function $g_i(\bar{x}_i)$ is positive and bounded, then there are two positive constants b_m and b_M, such that the following inequality holds

$$0 < b_m \leq g_i(\bar{x}_i) \leq b_M < \infty \tag{2}$$

Assumption 2 [14, 31] The reference signal y_d and $y_d^{(i)}, i = 1, \ldots, n$ are continuous and bounded, where $y_d^{(i)}$ denotes the i-th derivative of y_d. Furthermore, there exist constants $\bar{Y}_i \in R, i = 0, \ldots, n-1$ satisfying $y_d \leq \bar{Y}_0 < k_{c,1}(t)$ and $\bar{Y}_i < k_{c,i+1}(t)$.

2.2 Preliminaries

For the sake of simplicity, some basic concepts will be introduced based on the following stochastic nonlinear system

$$dx = f(\boldsymbol{x})dt + \hbar^{\mathrm{T}}(\boldsymbol{x})d\omega \tag{3}$$

where $\boldsymbol{x} \in R^n$ is the state of the system, ω is a r-dimensional standard Wiener process defined in complete probability space. $f(\boldsymbol{x}) : R^n \to R^n$ and $\hbar(\boldsymbol{x}) : R^n \to R^{n \times r}$ are local Lipschitz function with $f(\boldsymbol{0}) = 0$ and $\hbar(\boldsymbol{0}) = 0$.

Definition 1 [32] Considering system (3), for any second-order continuous differentiable function $V(\boldsymbol{x})$, define a differential operator L as follows:

$$LV(\boldsymbol{x}) = \frac{\partial V(\boldsymbol{x})}{\partial \boldsymbol{x}} f(\boldsymbol{x}) + \frac{1}{2} Tr\left\{\hbar^{\mathrm{T}} \frac{\partial^2 V(\boldsymbol{x})}{\partial \boldsymbol{x}^2} \hbar\right\} \tag{4}$$

where $Tr\{\bullet\}$ stands for the trace of matrix $\bullet$.

Definition 2 [15] Consider the stochastic nonlinear system (3) under a compact set $\Lambda \in R^n$ and the initial condition $\boldsymbol{x}_0 = \boldsymbol{x}(t_0)$. If there is always a constant $\tau > 0$ and a time constant $T = T(\tau, \boldsymbol{x}_0)$ such that $E[|\boldsymbol{x}(t)|^p] < \tau$ for all $t > t_0 + T$, then the state $\{\boldsymbol{x}(t), t \geq 0\}$ of (3) is said to be SGUUB in p-th moment.

Lemma 1 [8, 15] *On the basis of full consideration of the stochastic nonlinear system (3), if for $\forall \boldsymbol{x} \in R^n$ and $\forall t > t_0$, there exists $V(\boldsymbol{x}) \in C^2$, class K_∞ functions ζ_1 and ζ_2, and constants $\beta_0 > 0$ and $\gamma > 0$ such that*

$$\zeta_1(|\boldsymbol{x}|) \leq LV(\boldsymbol{x}) \leq \zeta_2(|\boldsymbol{x}|) \tag{5}$$

$$LV(\boldsymbol{x}) \leq -\beta_0 V(\boldsymbol{x}) + \gamma \tag{6}$$

then, system (3) has a unique strong solution for each $\boldsymbol{x}_0 \in R_n$ and satisfies

$$E[V(\boldsymbol{x})] \leq V(\boldsymbol{x}_0)e^{-\beta_0 t} + \frac{\gamma}{\beta_0}$$

2.3 Multi-dimensional Taylor network

In this paper, the unknown nonlinearity encountered in controller design will be approximated by MTNs, the structure diagram of MTN is shown in Fig. 1. More details about the MTN can be found in [20, 25, 35]. In brief, the following Lemma is introduced.

Lemma 2 [25, 35] *Let $\Phi(\boldsymbol{S}) : R^n \to R$ is a continuous function defined on a compact set Ω; for any $\sigma > 0$, there is always an MTN expressed as $\boldsymbol{\theta}^{\mathrm{T}} P_{m_n}(\boldsymbol{S})$ that can be used to approximate $\Phi(\boldsymbol{S})$ such that*

$$\Phi(\boldsymbol{S}) = \boldsymbol{\theta}^{\mathrm{T}} P_{m_n}(\boldsymbol{S}) + \delta(\boldsymbol{S}) \tag{7}$$

where $\delta(\boldsymbol{S})$ is the approximation error with $|\delta(\boldsymbol{S})| \leq \sigma$. In addition, $\boldsymbol{S} = [s_1, \ldots, s_n]^{\mathrm{T}} \in R^n$ and $\boldsymbol{\theta} = [\theta_1, \ldots, \theta_l]^{\mathrm{T}} \in R^l$ represent the input vector and weight vector of MTN,

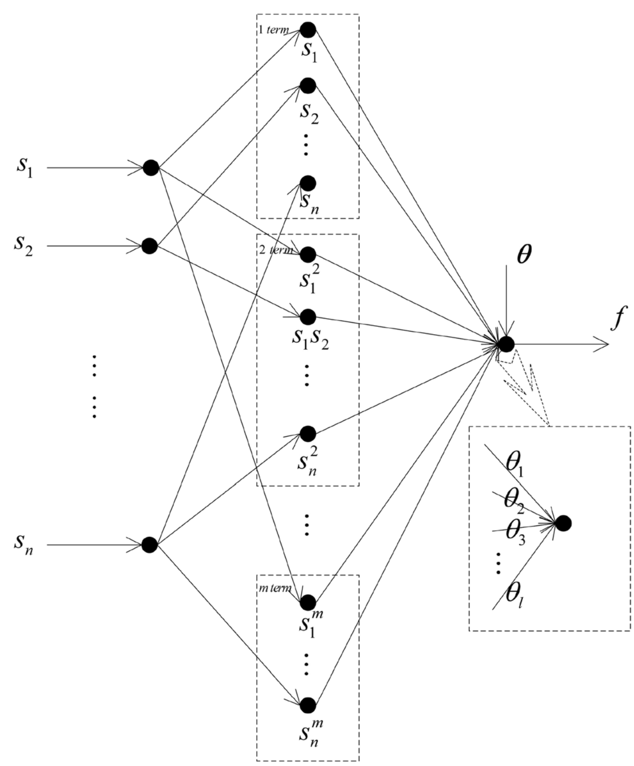

Fig. 1 Structure diagram of MTN

respectively.

$$P_{m_n}(\boldsymbol{S}) = [s_1, \ldots, s_n, s_1^2, \ldots, s_1 s_n, s_2^2, \ldots, s_n^2, s_1^m, \ldots, s_n^m]^{\mathrm{T}} \in R^l$$

is the middle layer of MTN. n and l are the dimension of the input layer and the middle layer, respectively.

Remark 1 MTN, like a radial basis function neural network (RBFNN), is a three-layer feedforward network with the key distinction being the design of the middle layer. MTN provides several advantages beyond other networks, including simple structure, small computation, and fast approximation speed. Firstly, MTN only performs addition and multiplication computations in the middle layer, and its output layer is a linear weighted combination, simplifying the structure of MTN and reducing computing costs. Secondly, PID and linear control are both special cases of MTN control, which can be employed as the initial values of MTN control to ensure the stability of the closed-loop system. Finally, MTN has the same learning ability as a RBFNN, and its basic structure efficiently decreases the complexity of the nonlinear mapping function in the middle layer, thereby lowering training time and expediting convergence.

2.4 Prescribed performance

According to [42], the prescribed performance is achieved by ensuring that the tracking error z_1 evolves within the following performance bounds

$$-\rho(t) < z_1(t) < \rho(t), \forall t \geq 0 \tag{8}$$

The term $\rho(t): R_+ \to R_+$ in (8) is a prescribed performance function, which is expressed as follows:

$$\rho(t) = (\rho_0 - \rho_\infty)e^{-\ell t} + \rho_\infty \tag{9}$$

where ρ_0, ρ_∞ and ℓ are positive design parameters. As mentioned in [42], $\rho(t)$ is a smooth and positive strictly decreasing function in $R_+ \to R_+$ and satisfies $\lim_{t\to\infty} \rho(t) = \rho_\infty$.

In order to design the tracking controller with prescribed performance, the following definition is given

$$z_1(t) = \rho(t)\overline{\lambda}(\varepsilon) \tag{10}$$

where ε is transformation error z_1 which is defined as $x_1 - y_d$, $\overline{\lambda}(\varepsilon) \in C^2$ is a function of ε and here we take it as hyperbolic tangent function as follows:

$$\overline{\lambda}(\varepsilon) = (e^{\varepsilon} - e^{-\varepsilon})/(e^{\varepsilon} + e^{-\varepsilon}) \tag{11}$$

According to (11), the following equation can be easily obtained

$$\varepsilon = 0.5\ln(\rho + z_1) - 0.5\ln(\rho - z_1) \tag{12}$$

Further, we can calculate derivative of ε as follows

$$d\varepsilon = S\big(dz_1 - \dot{\rho}(t)\overline{\lambda}(\varepsilon)dt\big) \tag{13}$$

where $S = 1/\left(\rho(t)\frac{\partial\overline{\lambda}}{\partial\varepsilon}\right) = \frac{e^{2\varepsilon}+2+e^{-2\varepsilon}}{4\rho(t)}$.

Based on the above discussion, it is easy to prove that the following inequality holds

$$S > \frac{1}{\rho(t)} \geq \frac{1}{\rho_0} > 0 \tag{14}$$

3 Main results

In this section, an adaptive prescribed performance tracking control scheme will be designed by combining backstepping technique and MTN approach. The control design is preceded by the following coordinate transformation

$$\begin{cases} \varepsilon = x_1 - y_d \\ z_i = x_i - \alpha_{i-1} \\ i = 2, \ldots, n \end{cases} \tag{15}$$

where α_{i-1} are intermediate virtual control signals, which will be designed in the backstepping process.

Remark 2 For simplicity, the variables are omitted from the corresponding functions. For example, $f_i(\bar{\boldsymbol{x}}_i)$ is abbreviated as f_i, $g_i(\bar{\boldsymbol{x}}_i)$ is abbreviated as g_i and $\phi_i^{\mathrm{T}}(\bar{\boldsymbol{x}}_i)$ is abbreviated as ϕ_i^{T}.

3.1 Controller design

Step 1: According to (15) and (13), the derivative of ε with respect to time t is obtained as follows:

$$d\varepsilon = S\big(f_1 + g_1 x_2 - \dot{y}_d - \dot{\rho}(t)\overline{\lambda}(\varepsilon)\big)dt + S\phi_1^{\mathrm{T}} d\omega \tag{16}$$

Selecting the first candidate tan-TVBLF as follows:

$$V_1 = \frac{k_{b,1}^4}{\pi}\tan\frac{\pi\varepsilon_1^4}{4k_{b,1}^4} + \frac{1}{2}\tilde{\boldsymbol{\theta}}_1^{\mathrm{T}}\tilde{\boldsymbol{\theta}}_1 \tag{17}$$

where $\tilde{\boldsymbol{\theta}}_1 = \boldsymbol{\theta}_1 - \hat{\boldsymbol{\theta}}_1$ is parameter error, $k_{b,1} = k_{c,1} - \bar{Y}_0$ and $|\varepsilon| \leq k_{b,1}$.

According to Definition 1, the derivative of V_1 is calculated as follows:

$$
\begin{aligned}
LV_1 = {} & \varepsilon^3\left(S\left(f_1 + g_1 x_2 - \dot{y}_d - \dot{\rho}(t)\overline{\lambda}(\varepsilon)\right)\right)\sec^2\frac{\pi\varepsilon^4}{4k_{b,1}^4} \\
& + \frac{3}{2}\varepsilon^2 \sec^2\frac{\pi\varepsilon^4}{4k_{b,1}^4}\left\|S\phi_1^{\mathrm{T}}\right\|^2 \\
& + \frac{\pi\varepsilon^6}{k_{b,1}^4}\tan\frac{\pi\varepsilon^4}{4k_{b,1}^4}\sec^2\frac{\pi\varepsilon^4}{4k_{b,1}^4}\left\|S\phi_1^{\mathrm{T}}\right\|^2 - \tilde{\boldsymbol{\theta}}_1^{\mathrm{T}}\dot{\hat{\boldsymbol{\theta}}}_1
\end{aligned} \tag{18}
$$

From the coordinate transformation (15), (18) can be calculated as follows:

$$
\begin{aligned}
LV_1 = {} & \varepsilon^3\left(S\left(f_1 + g_1 \alpha_1 - \dot{y}_d - \dot{\rho}(t)\overline{\lambda}(\varepsilon)\right)\right)\sec^2\frac{\pi\varepsilon^4}{4k_{b,1}^4} \\
& + S\varepsilon^3 g_1 z_2 \sec^2\frac{\pi\varepsilon^4}{4k_{b,1}^4} \\
& + \frac{3}{2}\varepsilon^2 \sec^2\frac{\pi\varepsilon^4}{4k_{b,1}^4}\left\|S\phi_1^{\mathrm{T}}\right\|^2 + \frac{\pi\varepsilon^6}{k_{b,1}^4}\tan\frac{\pi\varepsilon^4}{4k_{b,1}^4}\sec^2 \\
& \frac{\pi\varepsilon^4}{4k_{b,1}^4}\left\|S\phi_1^{\mathrm{T}}\right\|^2 - \tilde{\boldsymbol{\theta}}_1^{\mathrm{T}}\dot{\hat{\boldsymbol{\theta}}}_1
\end{aligned} \tag{19}
$$

By using Young's inequality, the following inequalities hold

$$
S\varepsilon^3 g_1 z_2 \sec^2\frac{\pi\varepsilon^4}{4k_{b,1}^4} \le \frac{1}{4}g_1 z_2^4 + \frac{3}{4}S^{\frac{4}{3}} g_1 \varepsilon^4 \sec^{\frac{8}{3}}\frac{\pi\varepsilon^4}{4k_{b,1}^4} \tag{20}
$$

$$
\frac{3}{2}\varepsilon^2 \sec^2\frac{\pi\varepsilon^4}{4k_{b,1}^4}\left\|S\phi_1^{\mathrm{T}}\right\|^2 \le \frac{3}{4}\tau_1^2 + \frac{3}{4\tau_1^2}\left\|S\phi_1^{\mathrm{T}}\right\|^4 \varepsilon^4 \sec^4\frac{\pi\varepsilon^4}{4k_{b,1}^4} \tag{21}
$$

where $\tau_1 > 0$ is a constant.

Substituting (20) and (21) into (19), the following inequality can be obtained as correct

$$
\begin{aligned}
LV_1 \le {} & \varepsilon^3 S(\bar{f}_1 + g_1\alpha_1)\sec^2\frac{\pi\varepsilon^4}{4k_{b,1}^4} + \frac{1}{4}g_1 z_2^4 \\
& + \frac{3}{4}\tau^2 - \frac{1}{2}S^2\varepsilon^6 \sec^4\frac{\pi\varepsilon^4}{4k_{b,1}^4} - \tilde{\boldsymbol{\theta}}_1^{\mathrm{T}}\dot{\hat{\boldsymbol{\theta}}}_1
\end{aligned} \tag{22}
$$

where $\bar{f}_1 = f_1 - \dot{y}_d - \dot{\rho}(t)\overline{\lambda}(\varepsilon) + \frac{1}{S}\left(\frac{\pi\varepsilon^3}{k_{b,1}^4}\tan\frac{\pi\varepsilon^4}{4k_{b,1}^4}\left\|S\phi_1^{\mathrm{T}}\right\|^2 + \frac{3}{4\tau_1^2}\left\|S\phi_1^{\mathrm{T}}\right\|^4\varepsilon\sec^2\frac{\pi\varepsilon^4}{4k_{b,1}^4}\right) + \frac{1}{2}S\varepsilon^3\sec^2\frac{\pi\varepsilon^4}{4k_{b,1}^4} + \frac{3}{4}S^{\frac{1}{3}}g_1\varepsilon\sec^{\frac{2}{3}}\frac{\pi\varepsilon^4}{4k_{b,1}^4}$.

Since the unknown continuous function $\bar{f}_1$ cannot be directly used in the design of controller, according to Lemma 2, for any $\sigma_1 > 0$, $\bar{f}_1$ can be approximated by a MTN as follows:

$$
\bar{f}_1 = \boldsymbol{\theta}_1^{\mathrm{T}} P_{m_1}(z_1) + \delta_1(z_1), |\delta_1(z_1)| \le \sigma_1
$$

where $z_1 = [\varepsilon]^{\mathrm{T}}$ and $\delta_1(z_1)$ is the approximation error.

Then, the following inequality holds by applying Young's inequality

$$
\begin{aligned}
\varepsilon^3 S\bar{f}_1 \sec^2\frac{\pi\varepsilon^4}{4k_{b,1}^4} \le {} & \varepsilon^3 S\boldsymbol{\theta}_1^{\mathrm{T}}P_{m_1}\sec^2\frac{\pi\varepsilon^4}{4k_{b,1}^4} \\
& + \frac{1}{2}S^2\varepsilon^6\sec^4\frac{\pi\varepsilon^4}{4k_{b,1}^4} + \frac{1}{2}\sigma_1^2
\end{aligned} \tag{23}
$$

Furthermore, substituting (23) into (22), the derivative of V_1 can be calculated as follows:

$$
\begin{aligned}
LV_1 \le {} & \varepsilon^3 S\left(\boldsymbol{\theta}_1^{\mathrm{T}}P_{m_1} + g_1\alpha_1\right)\sec^2\frac{\pi\varepsilon^4}{4k_{b,1}^4} + \frac{1}{4}g_1 z_2^4 \\
& + \frac{3}{4}\tau_1^2 + \frac{1}{2}\sigma_1^2 - \tilde{\boldsymbol{\theta}}_1^{\mathrm{T}}\dot{\hat{\boldsymbol{\theta}}}_1
\end{aligned} \tag{24}
$$

According to Assumption 1 and (24), the first virtual control signal α_1 is designed as follows:

$$
\alpha_1 = -\frac{\upsilon_1 k_{b,1}^4}{\pi\varepsilon^3}\sin\frac{\pi\varepsilon^4}{4k_{b,1}^4}\cos\frac{\pi\varepsilon^4}{4k_{b,1}^4} - \frac{1}{b_m}\hat{\boldsymbol{\theta}}_1^{\mathrm{T}}P_{m_1} \tag{25}
$$

where $\upsilon_1 > 0$ is a design parameter.

Remark 3 According to L'Hopital's rule, the following equation holds:

$$
\lim_{\varepsilon\to 0}\left(-\frac{\upsilon_1 k_{b,1}^4}{\pi\varepsilon^3}\sin\frac{\pi\varepsilon^4}{4k_{b,1}^4}\cos\frac{\pi\varepsilon^4}{4k_{b,1}^4}\right) = 0
$$

Therefore, there is no singularity in the virtual control signal α_1.

Substituting (25) into (24), the following inequality is established:

$$
\begin{aligned}
LV_1 \le {} & \Delta_1 + \tilde{\boldsymbol{\theta}}_1^{\mathrm{T}}\left(\varepsilon^3 SP_{m_1}\sec^2\frac{\pi\varepsilon^4}{4k_{b,1}^4} - \dot{\hat{\boldsymbol{\theta}}}_1\right) \\
& + \frac{1}{4}g_1 z_2^4 + \frac{3}{4}\tau_1^2 + \frac{1}{2}\sigma_1^2
\end{aligned} \tag{26}
$$

where $\Delta_1 = -\upsilon_1 b_m S\frac{k_{b1}^4}{\pi}\tan\frac{\pi\varepsilon^4}{4k_{b,1}^4}$.

Then, the adaptive law can be constructed as follows:

$$
\dot{\hat{\boldsymbol{\theta}}}_1 = -\eta_1\hat{\boldsymbol{\theta}}_1 + \varepsilon^3 SP_{m_1}\sec^2\frac{\pi\varepsilon^4}{4k_{b,1}^4} \tag{27}
$$

where η_1 is a positive constant.

Substituting the adaptive law (27) into (26), the following equation is obtained:

$$
LV_1 \le \Delta_1 + \frac{1}{4}g_1 z_2^4 + \frac{3}{4}\tau_1^2 + \frac{1}{2}\sigma_1^2 + \eta_1\tilde{\boldsymbol{\theta}}_1^{\mathrm{T}}\hat{\boldsymbol{\theta}}_1 \tag{28}
$$

Step 2: According to $z_2 = x_2 - \alpha_1$, the derivative of z_2 can be obtained as follows:

$$
dz_2 = (f_2 + g_2 x_3 - L\alpha_1)dt + \left(\phi_2 - \frac{\partial\alpha_1}{\partial x_1}\phi_2\right)^{\mathrm{T}} d\omega \tag{29}
$$

where $L\alpha_1 = \frac{\partial\alpha_1}{\partial x_1}(f_1 + g_1 x_2) + \sum_{j=0}^{1}\frac{\partial\alpha_1}{\partial y_d}y_d^{(j+1)} + \frac{\partial\alpha_1}{\partial\hat{\boldsymbol{\theta}}_1}\dot{\hat{\boldsymbol{\theta}}}_1 +$

$\frac{1}{2}\frac{\partial^2\alpha_1}{\partial x_1^2}\phi_1^{\mathrm{T}}\phi_1$, and $\alpha_1 \le \bar{Y}_1$.

Consider the second tan-TVBLF as follows:

$$V_2 = V_1 + \frac{k_{b,2}^4}{\pi}\tan\frac{\pi z_2^4}{4k_{b,2}^4} + \frac{1}{2}\tilde{\boldsymbol{\theta}}_2^{\mathrm{T}}\tilde{\boldsymbol{\theta}}_2 \tag{30}$$

where $\tilde{\boldsymbol{\theta}}_2 = \boldsymbol{\theta}_2 - \hat{\boldsymbol{\theta}}_2$ represents the parameter error and $k_{b,2} = k_{c,2} - \bar{Y}_1$.

In compact set Ω_{x_2}, take $x_3 = z_3 + \alpha_2$ into account, we have

$$\begin{aligned} LV_2 = LV_1 &+ z_2^3(f_2 + g_2\alpha_2 - L\alpha_1)\sec^2\frac{\pi z_2^4}{4k_{b,2}^4} \\ &+ \frac{3}{2}z_2^2\sec^2\frac{\pi z_2^4}{4k_{b,2}^4}\left\|\phi_2 - \frac{\partial\alpha_1}{\partial x_1}\phi_2\right\|^2 \\ &+ z_2^3 g_2 z_3\sec^2\frac{\pi z_2^4}{4k_{b,2}^4} \\ &+ \frac{\pi z_2^6}{k_{b,2}^4}\tan\frac{\pi z_2^4}{4k_{b,2}^4}\sec^2\frac{\pi z_2^4}{4k_{b,2}^4}\left\|\phi_2 - \frac{\partial\alpha_1}{\partial x_1}\phi_2\right\|^2 - \tilde{\boldsymbol{\theta}}_2^{\mathrm{T}}\dot{\hat{\boldsymbol{\theta}}}_2 \end{aligned} \tag{31}$$

Using Young's inequality, the following inequalities are easily obtained:

$$\begin{aligned} &\frac{3}{2}z_2^2\sec^2\frac{\pi z_2^4}{4k_{b,2}^4}\left\|\phi_2 - \frac{\partial\alpha_1}{\partial x_1}\phi_2\right\|^2 \\ &\le \frac{3}{4}\tau_2^2 + \frac{3}{4\tau_2^2}z_2^4\left\|\phi_2 - \frac{\partial\alpha_1}{\partial x_1}\phi_2\right\|^4\sec^4\frac{\pi z_2^4}{4k_{b,2}^4} \end{aligned} \tag{32}$$

$$z_2^3 g_2 z_3\sec^2\frac{\pi z_2^4}{4k_{b,2}^4} \le \frac{1}{4}g_2 z_3^4 + \frac{3}{4}g_2 z_2^4\sec^{\frac{8}{3}}\frac{\pi z_2^4}{4k_{b,2}^4} \tag{33}$$

where $\tau_2 > 0$ is a constant.

Substituting (32) and (33) into (31) yields

$$\begin{aligned} LV_2 \le\ & z_2^3(\bar{f}_2 + g_2\alpha_2)\sec^2\frac{\pi z_2^4}{4k_{b,2}^4} + \frac{3}{4}\tau_2^2 + \frac{1}{4}g_2 z_3^4 \\ &- \frac{1}{2}z_2^6\sec^4\frac{\pi z_2^4}{4k_{b,2}^4} \\ &- \tilde{\boldsymbol{\theta}}_2^{\mathrm{T}}\dot{\hat{\boldsymbol{\theta}}}_2 + \Delta_1 + \frac{3}{4}\tau_1^2 + \frac{1}{2}\sigma_1^2 + \eta_1\tilde{\boldsymbol{\theta}}_1^{\mathrm{T}}\hat{\boldsymbol{\theta}}_1 \end{aligned} \tag{34}$$

where $\bar{f}_2 = f_2 - L\alpha_1 + \frac{3}{4\tau_2^2}z_2\left\|\phi_2 - \frac{\partial\alpha_1}{\partial x_1}\phi_2\right\|^4\sec^2\frac{\pi z_2^4}{4k_{b,2}^4} + \frac{\pi z_2^3}{k_{b,2}^4}\tan\frac{\pi z_2^4}{4k_{b,2}^4}\left\|\phi_2 - \frac{\partial\alpha_1}{\partial x_1}\phi_2\right\|^2 + \frac{1}{4}g_1 z_2 + \frac{3}{4}g_2 z_2\sec^{\frac{8}{3}}\frac{\pi z_2^4}{4k_{b,2}^4} + \frac{1}{2}z_2^3\sec^2\frac{\pi z_2^4}{4k_{b,2}^4}$.

Obviously, $\bar{f}_2$ is an unknown nonlinear function, and according to Lemma 2, $\bar{f}_2$ can be approximated by a MTN with form $\boldsymbol{\theta}_2^{\mathrm{T}}P_{m_2}(z_2)$. That is to say, for any $\sigma_2 > 0$, there is

$$\bar{f}_2 = \boldsymbol{\theta}_2^{\mathrm{T}}P_{m_2}(z_2) + \delta(z_2),\ \ |\delta_2(z_2)| \le \sigma_2$$

where $z_2 = [\varepsilon, z_2]^{\mathrm{T}}$ and $\delta_2(z_2)$ is the approximation error.

Then by employing Yang's inequality, the following inequality holds:

$$z_2^3\bar{f}_2\sec^2\frac{\pi z_2^4}{4k_{b,2}^4} \le z_2^3\boldsymbol{\theta}_2^{\mathrm{T}}P_{m_2}\sec^2\frac{\pi z_2^4}{4k_{b,2}^4} + \frac{1}{2}z_2^6\sec^4\frac{\pi z_2^4}{4k_{b,2}^4} + \frac{1}{2}\sigma_2^2 \tag{35}$$

By substituting (35) into (34), (34) can be expressed as follows:

$$\begin{aligned} LV_2 \le\ & z_2^3(\boldsymbol{\theta}_2^{\mathrm{T}}P_{m_2} + g_2\alpha_2)\sec^2\frac{\pi z_2^4}{4k_{b,2}^4} + \frac{1}{2}\sigma_2^2 + \frac{3}{4}\tau_2^2 + \frac{1}{4}g_2 z_3^4 \\ &- \tilde{\boldsymbol{\theta}}_2^{\mathrm{T}}\dot{\hat{\boldsymbol{\theta}}}_2 + \Delta_1 + \frac{3}{4}\tau_1^2 + \frac{1}{2}\sigma_1^2 + \eta_1\tilde{\boldsymbol{\theta}}_1^{\mathrm{T}}\hat{\boldsymbol{\theta}}_1 \end{aligned} \tag{36}$$

According to (36) and Assumption 1, the virtual control signal α_2 is designed as follows:

$$\alpha_2 = -\frac{\upsilon_2 k_{b,2}^4}{\pi z_2^3}\sin\frac{\pi z_2^4}{4k_{b,2}^4}\cos\frac{\pi z_2^4}{4k_{b,2}^4} - \frac{1}{b_m}\hat{\boldsymbol{\theta}}_2^{\mathrm{T}}P_{m_2} \tag{37}$$

where $\upsilon_2 > 0$ is design parameter.

Substituting (37) into (36), the following inequality is easily obtained

$$\begin{aligned} LV_2 \le\ & \sum\nolimits_{j=1}^{2}\left(\Delta_j + \frac{1}{2}\sigma_j^2 + \frac{3}{4}\tau_j^2\right) + \frac{1}{4}g_2 z_3^4 \\ &+ \tilde{\boldsymbol{\theta}}_2^{\mathrm{T}}\left(z_2^3 P_{m_2}\sec^2\frac{\pi z_2^4}{4k_{b,2}^4} - \dot{\hat{\boldsymbol{\theta}}}_2\right) + \eta_1\tilde{\boldsymbol{\theta}}_1^{\mathrm{T}}\hat{\boldsymbol{\theta}}_1 \end{aligned} \tag{38}$$

where

$$\Delta_j = \begin{cases} -\upsilon_1 b_m S\dfrac{k_{b,1}^4}{\pi}\tan\dfrac{\pi\varepsilon^4}{4k_{b,1}^4}, & j = 1 \\ -\upsilon_j b_m\dfrac{k_{b,j}^4}{\pi}\tan\dfrac{\pi z_j^4}{4k_{b,j}^4}, & j = 2, \ldots, n \end{cases}$$

.

Remark 4 Based on the above description, the meaning of symbol Δ_j $j = 1, 2, \ldots, n$ will not be explained in the following steps.

According to (38), the following adaptive law can be established:

$$\dot{\hat{\boldsymbol{\theta}}}_2 = -\eta_2\hat{\boldsymbol{\theta}}_2 + z_2^3 P_{m_2}\sec^2\frac{\pi z_2^4}{4k_{b,2}^4} \tag{39}$$

where $\eta_2 > 0$ is a positive constant.

Substituting (39) into (38), we have

$$LV_2 \le \sum_{j=1}^{2}\left(\Delta_j + \frac{3}{4}\tau_j^2 + \frac{1}{2}\sigma_j^2 + \eta_j\tilde{\boldsymbol{\theta}}_j^{\mathrm{T}}\hat{\boldsymbol{\theta}}_j\right) + \frac{1}{4}g_2 z_3^4 \tag{40}$$

Step $3 \le i \le n-1$: According to $z_i = x_i - \alpha_{i-1}$, the derivative of z_i can be obtained

$$dz_i = (f_i + g_i x_{i+1} - L\alpha_{i-1})dt + \left(\phi_i - \sum_{j=1}^{i-1}\frac{\partial\alpha_{i-1}}{\partial x_j}\phi_j\right)^{\mathrm{T}} d\omega \tag{41}$$

where $L\alpha_{i-1} = \sum_{j=1}^{i-1}\frac{\partial\alpha_{i-1}}{\partial x_j}\left(f_j + g_j x_{j+1}\right) + \sum_{j=0}^{i-1}\frac{\partial\alpha_{i-1}}{\partial y_d^{(j)}}y_d^{(j+1)} + \frac{1}{2}\sum_{p,q=1}^{i-1}\frac{\partial^2\alpha_{i-1}}{\partial x_p x_q}\phi_p^{\mathrm{T}}\phi_q + \sum_{j=1}^{i-1}\frac{\partial\alpha_{i-1}}{\partial\hat{\boldsymbol{\theta}}_j}\dot{\hat{\boldsymbol{\theta}}}_j$ and $\alpha_i \le \bar{Y}_i$.

Consider the i-th tan-TVBLF as follows:

$$V_i = V_{i-1} + \frac{k_{b,i}^4}{\pi}\tan\frac{\pi z_i^4}{4k_{b,i}^4} + \frac{1}{2}\tilde{\boldsymbol{\theta}}_i^{\mathrm{T}}\tilde{\boldsymbol{\theta}}_i \tag{42}$$

where $\tilde{\boldsymbol{\theta}}_i = \boldsymbol{\theta}_i - \hat{\boldsymbol{\theta}}_i$ represents the parameter error and $k_{b,i} = k_{c,i} - \bar{Y}_{i-1}$.

According to Definition 1, the derivative of V_i is calculated as follows:

$$\begin{aligned} LV_i =& LV_{i-1} + z_i^3(f_i + g_i\alpha_i - L\alpha_{i-1})\sec^2\frac{\pi z_i^4}{4k_{b,i}^4} \\ &+ \frac{3}{2}z_i^2\sec^2\frac{\pi z_i^4}{4k_{b,i}^4}\left\|\phi_i - \sum_{j=1}^{i-1}\frac{\partial\alpha_{i-1}}{\partial x_j}\phi_j\right\|^2 + z_i^3 g_i z_{i+1}\sec^2\frac{\pi z_i^4}{4k_{b,i}^4} \\ &+ \frac{\pi z_i^6}{k_{b,i}^4}\tan\frac{\pi z_i^4}{4k_{b,i}^4}\sec^2\frac{\pi z_i^4}{4k_{b,i}^4}\left\|\phi_i - \sum_{j=1}^{i-1}\frac{\partial\alpha_{i-1}}{\partial x_j}\phi_j\right\|^2 - \tilde{\boldsymbol{\theta}}_i^{\mathrm{T}}\dot{\hat{\boldsymbol{\theta}}}_i \end{aligned} \tag{43}$$

Repeating the process in Step 2 for (43), the following inequality can be obtained:

$$LV_i \le \sum_{j=1}^{i}\left(\Delta_j + \frac{3}{4}\tau_j^2 + \frac{1}{2}\sigma_j^2 + \eta_j\tilde{\boldsymbol{\theta}}_j^{\mathrm{T}}\hat{\boldsymbol{\theta}}_j\right) + \frac{1}{4}g_i z_{i+1}^4 \tag{44}$$

The virtual control signal α_i and adaptive law $\dot{\hat{\boldsymbol{\theta}}}_i$ are designed as follows:

$$\alpha_i = -\frac{\upsilon_i k_{b,i}^4}{\pi z_i^3}\sin\frac{\pi z_i^4}{4k_{b,i}^4}\cos\frac{\pi z_i^4}{4k_{b,i}^4} - \frac{1}{b_m}\hat{\boldsymbol{\theta}}_i^{\mathrm{T}}P_{m_i} \tag{45}$$

$$\dot{\hat{\boldsymbol{\theta}}}_i = -\eta_i\hat{\boldsymbol{\theta}}_i + z_i^3 P_{m_i}\sec^2\frac{\pi z_i^4}{4k_{b,i}^4} \tag{46}$$

where $\upsilon_i > 0$ and $\eta_i > 0$ are design parameters.

Step n: According to $z_n = x_n - \alpha_{n-1}$, the derivative of z_n can be calculated as follows:

$$dz_n = (f_n + g_n u - L\alpha_{n-1})dt + \left(\phi_n - \sum_{j=1}^{n-1}\frac{\partial\alpha_{n-1}}{\partial x_j}\phi_j\right)^{\mathrm{T}} d\omega \tag{47}$$

where $L\alpha_{n-1} = \sum_{j=1}^{n-1}\frac{\partial\alpha_{n-1}}{\partial x_j}\left(f_j + g_j x_{j+1}\right) + \sum_{j=0}^{n-1}\frac{\partial\alpha_{n-1}}{\partial y_d^{(j)}}y_d^{(j+1)} + \frac{1}{2}\sum_{p,q=1}^{n-1}\frac{\partial^2\alpha_{n-1}}{\partial x_p x_q}\phi_p^{\mathrm{T}}\phi_q + \sum_{j=1}^{n-1}\frac{\partial\alpha_{n-1}}{\partial\hat{\boldsymbol{\theta}}_j}\dot{\hat{\boldsymbol{\theta}}}_j$.

Consider the n-th tan-TVBLF as follows:

$$V_n = V_{n-1} + \frac{k_{b,n}^4}{\pi}\tan\frac{\pi z_n^4}{4k_{b,n}^4} + \frac{1}{2}\tilde{\boldsymbol{\theta}}_n^{\mathrm{T}}\tilde{\boldsymbol{\theta}}_n \tag{48}$$

where $\tilde{\boldsymbol{\theta}}_n = \boldsymbol{\theta}_n - \hat{\boldsymbol{\theta}}_n$ represents the parameter error and $k_{b,n} = k_{c,n} - \bar{Y}_{n-1}$.

In the compact set Ω_{x_n}, according to Definition 1, the following inequality can be obtained:

$$\begin{aligned} LV_n =& LV_{n-1} + z_n^3(f_n + g_n u - L\alpha_{n-1})\sec^2\frac{\pi z_n^4}{4k_{b,n}^4} \\ &+ \frac{3}{2}z_n^2\sec^2\frac{\pi z_n^4}{4k_{b,n}^4}\left\|\phi_n - \sum_{j=1}^{n-1}\frac{\partial\alpha_{n-1}}{\partial x_j}\phi_j\right\|^2 \\ &+ \frac{\pi z_n^6}{k_{b,n}^4}\tan\frac{\pi z_n^4}{4k_{b,n}^4}\sec^2\frac{\pi z_n^4}{4k_{b,n}^4}\left\|\phi_n - \sum_{j=1}^{n-1}\frac{\partial\alpha_{n-1}}{\partial x_j}\phi_j\right\|^2 - \tilde{\boldsymbol{\theta}}_n^{\mathrm{T}}\dot{\hat{\boldsymbol{\theta}}}_n \end{aligned} \tag{49}$$

By applying Young's inequality, the following inequality is easily can be obtained:

$$\begin{aligned} &\frac{3}{2}z_n^2\sec^2\frac{\pi z_n^4}{4k_{b,n}^4}\left\|\phi_n - \sum_{j=1}^{n-1}\frac{\partial\alpha_{n-1}}{\partial x_j}\phi_j\right\|^2 \\ &\le \frac{3}{4}\tau_n^2 + \frac{3}{4\tau_n^2}z_n^4\left\|\phi_n - \sum_{j=1}^{n-1}\frac{\partial\alpha_{n-1}}{\partial x_j}\phi_j\right\|^4\sec^4\frac{\pi z_n^4}{4k_{b,n}^4} \end{aligned} \tag{50}$$

where $\tau_n > 0$ is a constant.

Substitute (50) into (49) to get the following inequality:

$$\begin{aligned} LV_n \le& \sum_{j=1}^{n-1}\left(\Delta_j + \frac{3}{4}\tau_j^2 + \frac{1}{2}\sigma_j^2 + \eta_j\tilde{\boldsymbol{\theta}}_j^{\mathrm{T}}\hat{\boldsymbol{\theta}}_j\right) - \frac{1}{2}z_n^6\sec^4\frac{\pi z_n^4}{4k_{b,n}^4} \\ &+ z_n^3(\bar{f}_n + g_n u)\sec^2\frac{\pi z_n^4}{4k_{b,n}^4} + \frac{3}{4}\tau_n^2 - \tilde{\boldsymbol{\theta}}_n^{\mathrm{T}}\dot{\hat{\boldsymbol{\theta}}}_n \end{aligned} \tag{51}$$

where $\bar{f}_n = f_n - L\alpha_{n-1} + \frac{3}{4\tau_n^2}z_n\left\|\phi_n - \sum_{j=1}^{n-1}\frac{\partial\alpha_{n-1}}{\partial x_j}\phi_j\right\|^4\sec^2\frac{\pi z_n^4}{4k_{b,n}^4} + \frac{1}{2}z_n^3\sec^2\frac{\pi z_n^4}{4k_{b,n}^4} + \frac{\pi z_n^3}{k_{b,n}^4}\tan\frac{\pi z_n^4}{4k_{b,n}^4}\left\|\phi_n - \sum_{j=1}^{n-1}\frac{\partial\alpha_{n-1}}{\partial x_j}\phi_j\right\|^2 + \frac{1}{4}g_{n-1}z_n$.

Similarly, $\bar{f}_n$ cannot be used to design the controller; according to the conclusion of Lemma 2, $\bar{f}_n$ can be approximated by a MTN with form $\boldsymbol{\theta}_n^{\mathrm{T}}P_{m_n}(z_n)$. In particular, for any $\sigma_n > 0$, there is

$$\bar{f}_n = \boldsymbol{\theta}_n^{\mathrm{T}} P_{m_n}(z_n) + \delta(z_n),\ |\delta_n(z_n)| \le \sigma_n$$

where $z_n = [\varepsilon, z_2, \cdots, z_n]^{\mathrm{T}}$ and $\delta_n(z_n)$ is the approximation error.

Then, the following inequality holds:

$$z_n^3 \bar{f}_n \sec^2 \frac{\pi z_n^4}{4k_{b,n}^4} \le z_n^3 \boldsymbol{\theta}_n^{\mathrm{T}} P_{m_n} \sec^2 \frac{\pi z_n^4}{4k_{b,n}^4} + \frac{1}{2} z_n^6 \sec^4 \frac{\pi z_n^4}{4k_{b,n}^4} + \frac{1}{2}\sigma_n^2 \tag{52}$$

Combining (51) with (52), the following inequality is obtained:

$$\begin{aligned} LV_n \le & \sum\nolimits_{j=1}^{n-1} \left(\Delta_j + \frac{3}{4}\tau_j^2 + \frac{1}{2}\varepsilon_j^2 + \eta_j \tilde{\boldsymbol{\theta}}_j^{\mathrm{T}} \hat{\boldsymbol{\theta}}_j \right) - \tilde{\boldsymbol{\theta}}_n^{\mathrm{T}} \dot{\hat{\boldsymbol{\theta}}}_n \\ & + z_n^3 (\boldsymbol{\theta}_n^{\mathrm{T}} P_{m_n} + g_n u) \sec^2 \frac{\pi z_n^4}{4k_{b,n}^4} + \frac{1}{2}\sigma_n^2 + \frac{3}{4}\tau_n^2 \end{aligned} \tag{53}$$

According to (53), design the actual control input u as follows:

$$u = -\frac{\upsilon_n k_{b,n}^4}{\pi z_n^3} \sin \frac{\pi z_n^4}{4k_{b,n}^4} \cos \frac{\pi z_n^4}{4k_{b,n}^4} - \frac{1}{b_m} \hat{\boldsymbol{\theta}}_n^{\mathrm{T}} P_{m_n} \tag{54}$$

Substituting (54) into (53) yields

$$\begin{aligned} LV_n \le & \sum\nolimits_{j=1}^{n} \left(\Delta_j + \frac{3}{4}\tau_j^2 + \frac{1}{2}\sigma_j^2 + \eta_j \tilde{\boldsymbol{\theta}}_j^{\mathrm{T}} \hat{\boldsymbol{\theta}}_j \right) \\ & + \tilde{\boldsymbol{\theta}}_n^{\mathrm{T}} \left(z_n^3 P_{m_n} \sec^2 \frac{\pi z_n^4}{4k_{b,n}^4} - \dot{\hat{\boldsymbol{\theta}}}_n \right) \end{aligned} \tag{55}$$

Based on (55), the adaptive law is constructed according to (55) as follows:

$$\dot{\hat{\boldsymbol{\theta}}}_n = -\eta_n \hat{\boldsymbol{\theta}}_n + z_n^3 P_{m_n} \sec^2 \frac{\pi z_n^4}{4k_{b,n}^4} \tag{56}$$

Substituting (56) into (55), we have

$$LV_n \le \sum\nolimits_{j=1}^{n} \left(\Delta_j + \frac{3}{4}\tau_j^2 + \frac{1}{2}\sigma_j^2 + \eta_j \tilde{\boldsymbol{\theta}}_j^{\mathrm{T}} \hat{\boldsymbol{\theta}}_j \right) \tag{57}$$

3.2 Stability analysis

Theorem 1 *Under Assumptions* 1–2, *consider the whole closed-loop system consisting of the stochastic nonlinear system* (1), *the virtual control signals* (25), (37), (45) *and the actual control input* (54) *with the adaptive laws* (27), (39), (46), (56). *Then for any bounded initial condition, the following properties can be guaranteed*:

1) All signals in closed-loop system are SGUUB in probability.
2) The full state constraints is successfully implemented.
3) The system output y can effectively track the reference signal y_d and the tracking error is constrained within the prescribed performance boundary.

Proof For the considered closed-loop system, the following tan-TVBLF is constructed:

$$V = \sum_{i=1}^{n} \frac{k_{b,i}^4}{\pi} \tan \frac{\pi z_i^4}{4k_{b,i}^4} + \frac{1}{2} \sum_{i=1}^{n} \tilde{\boldsymbol{\theta}}_i^{\mathrm{T}} \tilde{\boldsymbol{\theta}}_i \tag{58}$$

According to (57) and (58), the following inequality can be obtained:

$$LV \le \sum_{i=1}^{n} \left(\Delta_i + \frac{3}{4}\tau_i^2 + \frac{1}{2}\varepsilon_i^2 + \eta_i \tilde{\boldsymbol{\theta}}_i^{\mathrm{T}} \hat{\boldsymbol{\theta}}_i \right) \tag{59}$$

where $\Delta_1 = -\upsilon_1 b_m S \frac{k_{b,1}^4}{\pi} \tan \frac{\pi \varepsilon^4}{4k_{b,1}^4}$, $\Delta_i = -\upsilon_i b_m \frac{k_{b,i}^4}{\pi} \tan \frac{\pi z_i^4}{4k_{b,i}^4}$ for $i = 2, 3, \ldots, n$, and $\upsilon_i > 0$ and $\eta_i > 0$ are design parameters for $i = 1, 2, \ldots, n$.

According to Young's inequality, and take $\tilde{\boldsymbol{\theta}}_i = \boldsymbol{\theta}_i - \hat{\boldsymbol{\theta}}_i$ into account, we have

$$\eta_i \tilde{\boldsymbol{\theta}}_i^{\mathrm{T}} \hat{\boldsymbol{\theta}}_i \le \eta_i \tilde{\boldsymbol{\theta}}_i^{\mathrm{T}} \left(\boldsymbol{\theta}_i - \tilde{\boldsymbol{\theta}}_i \right) \le -\frac{1}{2} \eta_i \tilde{\boldsymbol{\theta}}_i^{\mathrm{T}} \tilde{\boldsymbol{\theta}}_i + \frac{1}{2} \eta_i \boldsymbol{\theta}_i^2 \tag{60}$$

Then, combining (59) with (60), the following inequality can be obtained:

$$LV \le -\beta_0 V_n + \gamma \tag{61}$$

where $\beta_0 = \min\{\upsilon_1 b_m S, \upsilon_i b_m, \eta_i : i = 1, 2, \ldots, n\}$ and $\gamma = \frac{3}{4}\sum_{i=1}^{n} \tau_i^2 + \frac{1}{2}\sum_{i=1}^{n} \varepsilon_i^2 + \frac{1}{2}\sum_{i=1}^{n} \eta_i \boldsymbol{\theta}_i^2$.

According to (61), using Lemma 1, for any $t \ge 0$, the following inequality is easy to obtain

$$0 \le E[V(t)] \le V(0) e^{-\beta_0 t} + \frac{\gamma}{\beta_0} \tag{62}$$

On the one hand, inequality (62) indicates that $E[V(t)]$ is eventually bounded by γ/β_0. Thus, according to Definition 2 and recalling (58), it is easy to conclude that all signals of the closed-loop system are SGUUB in probability. Moreover, the controller design process shows that the tracking error is constrained within the prescribed performance boundary $\rho(t)$.

On the other hand, $y_d \le \bar{Y}_0 < k_{c,1}$ can be known from Assumption 2. Since $x_1 = \varepsilon + y_d$, $k_{b,i} = k_{c,i} - \bar{Y}_{i-1}$ and $|\varepsilon| \le k_{b,1}$, it is easy to get $|x_1| \le k_{c,1}$. Similarly, because of $x_i = z_i + \alpha_{i-1}$, $\alpha_{i-1} \le \bar{Y}_{i-1}$ and $k_{b,i} = k_{c,i} - \bar{Y}_{i-1}$, for $i = 2, \ldots, n$, it is easy to prove that $|x_i| \le k_{c,i}$. Therefore, it is concluded that the full state constraints in the closed-loop system are successfully implemented. □

4 Simulation examples

In this section, two simulation examples are provided to demonstrate the validity of the designed controller.

Example 1 (numerical example): Consider the following stochastic nonlinear system

$$\begin{cases} dx_1 = \left(-x_1 e^{-0.2x_1} + x_2\right)dt + 0.1x_1 d\omega \\ dx_2 = (2x_2 + u)dt + 0.05x_2 d\omega \\ \quad y = x_1 \end{cases} \tag{63}$$

with the initial value are selected as $x_1 = 0.1$, $x_2 = 0.1$, and the reference signal is selected as $y_d = 0.6\sin t$. According to Theorem 1, the virtual control signal, actual control input and adaptive laws are constructed as follows:

$$\alpha_1 = -\frac{\upsilon_1 k_{b,1}^4}{\pi\varepsilon^3}\sin\frac{\pi\varepsilon^4}{4k_{b,1}^4}\cos\frac{\pi\varepsilon^4}{4k_{b,1}^4} - \frac{1}{b_m}\hat{\boldsymbol{\theta}}_1^{\mathrm{T}} P_{m_1}$$

$$u = -\frac{\upsilon_2 k_{b,2}^4}{\pi z_2^3}\sin\frac{\pi z_2^4}{4k_{b,2}^4}\cos\frac{\pi z_2^4}{4k_{b,2}^4} - \frac{1}{b_m}\hat{\boldsymbol{\theta}}_2^{\mathrm{T}} P_{m_2}$$

$$\dot{\hat{\boldsymbol{\theta}}}_i = -\eta_i\hat{\boldsymbol{\theta}}_i + z_i^3 P_{m_i}\sec^2\frac{\pi z_i^4}{4k_{b,i}^4}, i = 1,2$$

In simulation, the parameters of $\rho(t)$ are designed as $\rho_0 = 2$, $\rho_\infty = 0.01$ and $\ell = 0.4$. The parameters of the controller are designed as $\eta_1 = 0.01$, $\eta_2 = 0.001$, $v_1 = 0.01$ and $v_2 = 0.001$. All states are constrained to be within the ranges $|x_1| \le 0.35\sin t + 1$ and $|x_2| \le 0.35\sin 0.5t + 1.5$. The simulation results are shown in Figs. 2, 3, 4, and 5.

Figure 2 shows the trajectory of the system output y is consistent with the trajectory of the reference signal y_d, which indicates that good tracking performance is achieved. Figure 3 illustrates the tracking error converges to a small neighborhood of origin, and it can be seen that the tracking error is constrained within the prescribed performance boundary. Figure 4 shows the trajectory of input u. Figure 5 demonstrates that the state x_2 is constrained within the specified range of time-varying state constraints. From the above simulation results, it can be seen that the proposed control scheme can ensure that all variables are bounded, and a satisfactory tracking effect is obtained.

Example 2 (Actual system example): To further illustrate the applicability of the proposed method, a class of Duffing–Holmes stochastic nonlinear system is considered. According to [47], the system can be expressed as follows:

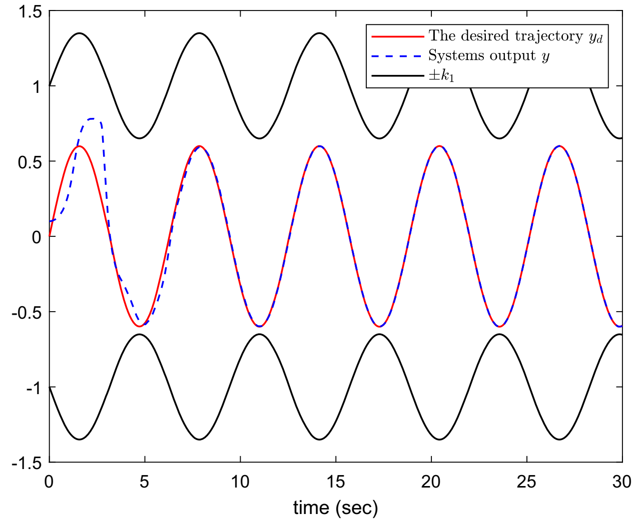

Fig. 2 Trajectories of y and y_d of Example 1

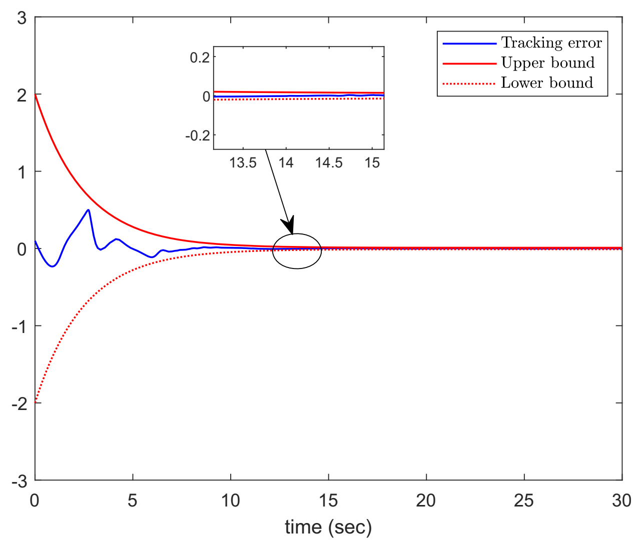

Fig. 3 Trajectories of tracking errors and prescribed performance boundary

$$\begin{cases} dx_1 = (x_1 + x_2)dt \\ dx_2 = (f_2(\bar{\boldsymbol{x}}_2) + u)dt + \phi_2(\bar{\boldsymbol{x}}_2)d\omega \\ \quad y = x_1 \end{cases} \tag{64}$$

where $f_2(\bar{\boldsymbol{x}}_2) = -x_1 - 0.25x_2 - x_1^3 + 0.3\cos(0.1t)$ and $\phi_2(\bar{\boldsymbol{x}}_2) = -0.02x_1^2\cos(0.1x_2)$. The initial values of the system and the reference signal are set as $x(0) = [0.1, 0.1]^{\mathrm{T}}$, $y_d = 0.6\sin t$, respectively.

Adopting the same control strategy as in Example 1 for system (64), the parameters of $\rho(t)$ are designed as $\rho_0 = 2$, $\rho_\infty = 0.01$ and $\ell = 0.4$. The states are constrained to $|x_1| \le 0.2\sin t + 1.3$ and $|x_2| \le 0.1\sin t + 4$. The

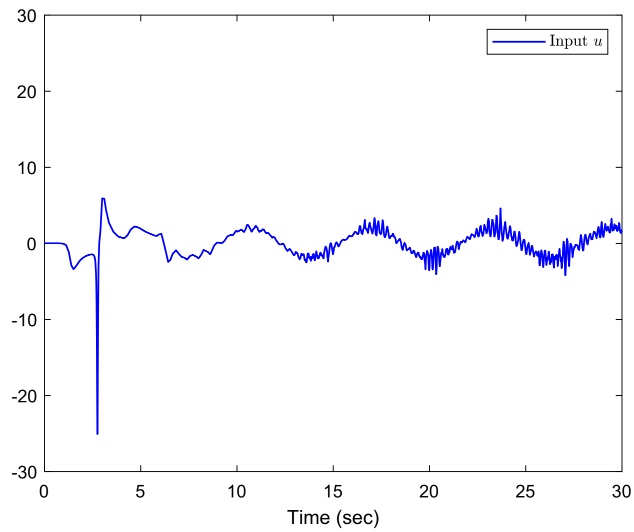

Fig. 4 Trajectories of the control input u of Example 1

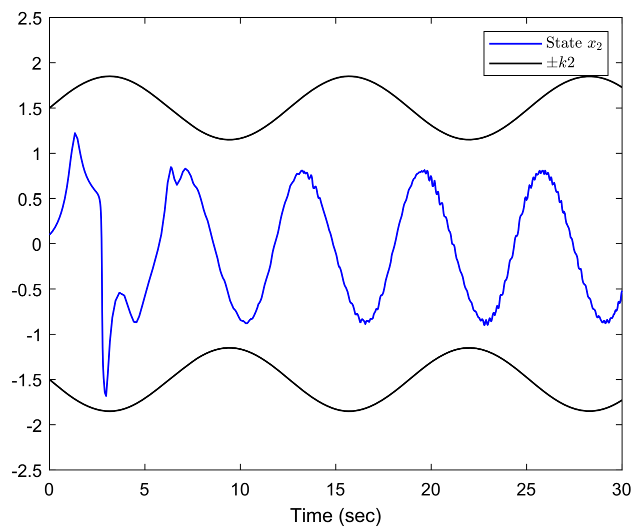

Fig. 5 Trajectories of states x_2 and its constrained boundaries

parameters of the controller are designed as $\eta_1 = 0.01$, $\eta_2 = 0.01$, $v_1 = 0.01$, $v_2 = 0.001$. The simulation results are shown in Figs. 6, 7, 8, 9.

Figure 6 shows the trajectories of output of the system y and the reference signal y_d, it can be seen that a good tracking performance is achieved. Figure 7 reveals that the tracking error of the system satisfies the prescribed constraints and the steady-state performance. Figures 8 and 9 show the trajectories of the input u and the state x_2, respectively. It can be observed that all states are constrained within the given region. The above results further illustrate the effectiveness of the proposed control approach.

Remark 5 In order to meet the performance constraint throughout the design process, a larger input must be given to the system when the error is large. This will also result in

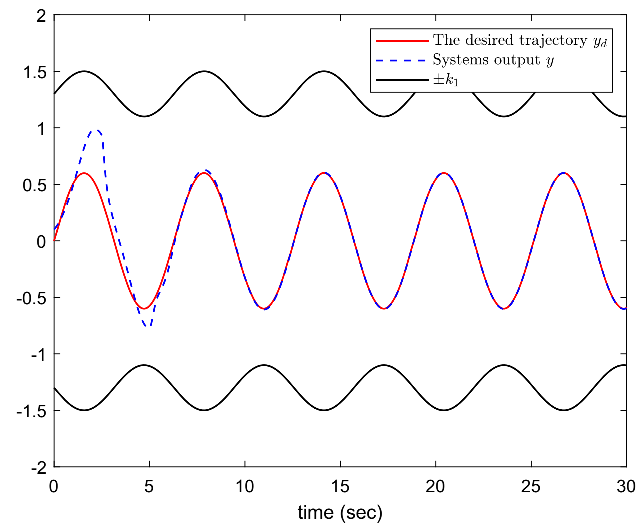

Fig. 6 Trajectories of y and y_d of Example 2

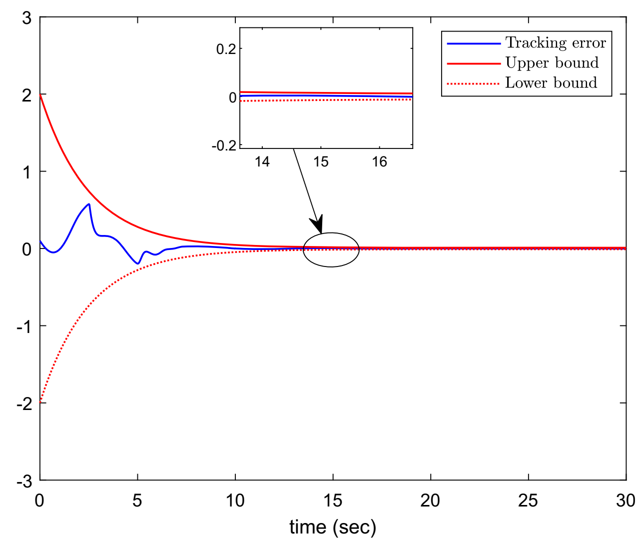

Fig. 7 Trajectories of tracking errors and prescribed performance boundary

a larger output from the system. This is the reason for the large fluctuation in the tracking trajectory.

Remark 6 The selection of parameters directly affects the control performance of the system. It can be known that the control strategy proposed in this paper contains several design parameters. The above simulation results show that the selection of suitable parameters leads to a satisfactory tracking effect of the controlled system.

Remark 7 Practical systems generally suffer from stochastic factors. Considering these disturbances can help improve the control accuracy and control performance. This conclusion is supported by [48]. In this paper, the effect of stochastic disturbances is considered in the system, which is more in line with the requirements of

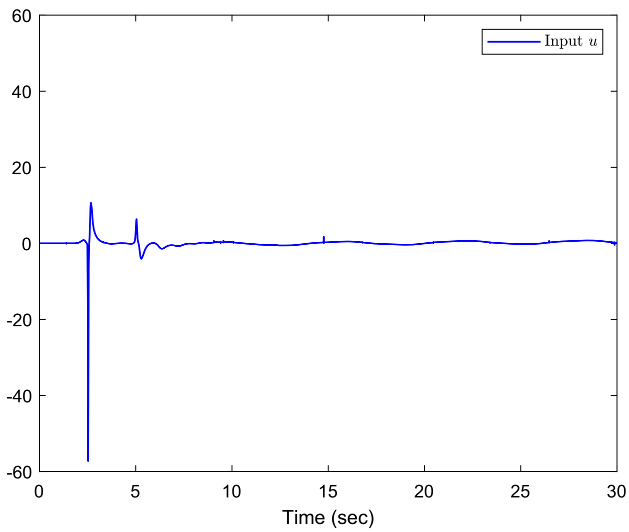

Fig. 8 Trajectories of the control input u of Example 2

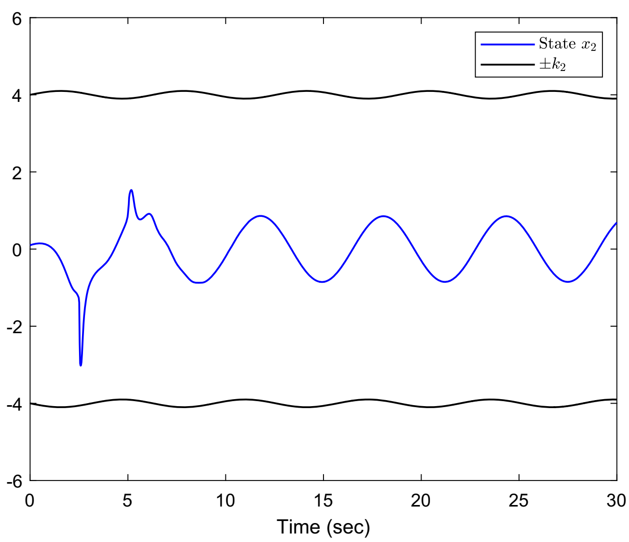

Fig. 9 Trajectories of states x_2 and its constrained boundaries

practical engineering. The simulation results reveal that the proposed control strategy produces good control performance, as demonstrated by the trajectories in Figs. 2, 3, 4, 5, 6, 7, 8, and 9.

5 Conclusion

In this paper, the adaptive tracking control issue under prescribed performance is investigated for a class of stochastic nonlinear systems with unknown control direction and full state constraints. The steady-state performance and transient performance of the system are simultaneously achieved by cleverly integrating the idea of PPC into the controller design. The constructed tan-TVBLFs ensure that all system states are limited within the specified range. According to Lyapunov stability theorem, it is proved that all signals are SGUUB in probability and the tracking error falls in a neighborhood of the origin. Two simulation examples fully verify the applicability and effectiveness of the proposed control strategy.

Funding This work was supported by the Shandong Provincial Natural Science Foundation, China (No. ZR2020QF055).

Data availability Data sharing is not applicable to this article as no new data were created or analyzed in this study.

Declarations

Conflict of interest The author(s) declare that they have no conflict of interest.

References

1. Yin JL, Khoo SY, Man ZH, Yu XH (2011) Finite-time stability and instability of stochastic nonlinear systems. Automatica 47(12):2671–2677
2. Li FZ, Liu YG (2014) Global stability and stabilization of more general stochastic nonlinear systems. J Math Anal Appl 413(2):841–855
3. Yao LQ, Zhang WH, Xie XJ (2020) Stability analysis of random nonlinear systems with time-varying delay and its application. Automatica 117:108994
4. Mahmood M, Mhaskar P (2012) Lyapunov-based model predictive control of stochastic nonlinear systems. Automatica 48(9):2271–2276
5. Mao XR (2002) A note on the LaSalle-type theorems for stochastic differential delay equations. J Math Anal Appl 268(1):125–142
6. Wu ZJ, Xie XJ, Shi P, Xia YQ (2009) Backstepping controller design for a class of stochastic nonlinear systems with Markovian switching. Automatica 45(4):997–1004
7. Zhang QL, Li L, Yan XG, Spurgeon SK (2017) Sliding mode control for singular stochastic markovian jump systems with uncertainties. Automatica 79:27–34
8. Liu SJ, Zhang JF, Jiang ZP (2007) Decentralized adaptive output-feedback stabilization for large-scale stochastic nonlinear systems. Automatica 43(2):238–251
9. Li WQ, Jing YW, Zhang SY (2011) Adaptive state-feedback stabilization for a large class of high-order stochastic nonlinear systems. Automatica 47(4):819–828
10. Ji HB, Xi HS (2006) Adaptive output-feedback tracking of stochastic nonlinear systems. IEEE Trans Autom Control 51(2):355–360
11. Wu ZJ, Xie XJ, Zhang SY (2007) Adaptive backstepping controller design using stochastic small-gain theorem. Automatica 43(4):608–620
12. Su H, Zhang WH (2020) Adaptive fuzzy control of stochastic nonlinear systems with fuzzy dead zones and unmodeled dynamics. IEEE Trans Cybern 50(2):587–599
13. Lu YK (2018) Adaptive-fuzzy control compensation design for direct adaptive fuzzy control. IEEE Trans Fuzzy Syst 26(6):3222–3231
14. Wang HQ, Chen B, Lin C (2014) Adaptive neural tracking control for a class of stochastic nonlinear systems. Int J Robust Nonlinear Control 24(7):1262–1280

15. Chen WS, Jiao LC, Du ZB (2010) Output-feedback adaptive dynamic surface control of stochastic non-linear systems using neural network. IET Control Theory Appl 4(12):3012–3021
16. Li HY, Wang LJ, Du HP, Boulkroune A (2017) Adaptive fuzzy backstepping tracking control for strict-feedback systems with input delay. IEEE Trans Fuzzy Syst 25(3):642–652
17. Sui S, Tong SC, Li YM (2014) Adaptive fuzzy backstepping output feedback tracking control of MIMO stochastic pure-feedback nonlinear systems with input saturation. Fuzzy Sets Syst 254:26–46
18. Sun YM, Chen B, Lin C, Wang HH, Zhou SW (2016) Adaptive neural control for a class of stochastic nonlinear systems by backstepping approach. Inf Sci 369:748–764
19. Liu H, Pan YP, Cao JD, Wang HX, Zhou Y (2020) Adaptive neural network backstepping control of fractional-order nonlinear systems with actuator faults. IEEE Trans Neural Netw Learn Syst 31(12):5166–5177
20. Han YQ, Zhu SL, Yang SG, Chu L (2021) Adaptive multi-dimensional Taylor network tracking control for a class of non-linear systems. Int J Control 94(2):277–285
21. Sun QM, Yan HS (2020) Multi-dimensional Taylor network modelling and optimal control of SISO nonlinear systems for tracking by output feedback. IMA J Math Control Inf 37(3):699–717
22. Yan HS, Kang AM (2017) Asymptotic tracking and dynamic regulation of SISO non-linear system based on discrete multi-dimensional Taylor network. IET Control Theory Appl 11(10):1619–1626
23. Yan HS, Sun QM (2021) MTN output feedback tracking control for MIMO discrete-time uncertain nonlinear systems. ISA Trans 111:71–81
24. Zhang C, Yan HS (2020) Multidimensional Taylor network adaptive control for MIMO time-varying uncertain nonlinear systems with noises. Int J Robust Nonlinear Control 30(1):397–420
25. Han YQ, Yan HS (2018) Adaptive multi-dimensional Taylor network tracking control for SISO uncertain stochastic non-linear systems. IET Control Theory Appl 12(8):1107–1115
26. Yan HS, Han YQ, Sun QM (2018) Optimal output-feedback tracking of SISO stochastic nonlinear systems using multi-dimensional Taylor network. Trans Inst Measur Control 40(10):3049–3058
27. Wang MX, Zhu SL, Liu SM, Du Y, Han YQ (2023) Design of adaptive finite-time fault-tolerant controller for stochastic non-linear systems with multiple faults. IEEE Trans Autom Sci Eng 20(4):2492–2502. https://doi.org/10.1109/TASE.2022.3206328
28. Gao YF, Sun XM, Wen CY, Wang W (2017) Adaptive tracking control for a class of stochastic uncertain nonlinear systems with input saturation. IEEE Trans Autom Control 62(5):2498–2504
29. Min HF, Xu SY, Zhang BY, Ma Q (2019) Output-feedback control for stochastic nonlinear systems subject to input saturation and time-varying delay. IEEE Trans Autom Control 64(1):359–364
30. Wang HQ, Liu XP, Liu KF, Karimi HR (2015) Approximation-based adaptive fuzzy tracking control for a class of nonstrict-feedback stochastic nonlinear time-delay systems. IEEE Trans Fuzzy Syst 23(5):1746–1760
31. Gao TT, Liu YJ, Li DP, Tong SC, Li TS (2021) Adaptive neural control using tangent time-varying BLFs for a class of uncertain stochastic nonlinear systems with full state constraints. IEEE Transactions on Cybernetics 51(4):1943–1953
32. Liu YJ, Lu SM, Tong SC, Chen XK, Chen CLP, Li DJ (2018) Adaptive control-based barrier Lyapunov functions for a class of stochastic nonlinear systems with full state constraints. Automatica 87:83–93
33. Zhu QD, Liu YC (2021) Neural network adaptive finite-time control of stochastic nonlinear systems with full state constraints. Asian J Control 23(4):1728–1739
34. Han YQ (2022) Adaptive control of a class of stochastic nonlinear systems with full state constraints and input saturation using multi-dimensional Taylor network. Asian J Control 24(4):1609–1621
35. Li N, Han YQ, He WJ, Zhu SL (2022) Control design for stochastic nonlinear systems with full-state constraints and input delay: a new adaptive approximation method. Int J Control Autom Syst 20(8):2768–2778
36. Zhou Q, Li HY, Wang LJ, Lu RQ (2018) Prescribed performance observer-based adaptive fuzzy control for nonstrict-feedback stochastic nonlinear systems. IEEE Trans Syst Man Cybern Syst 48(10):1747–1758
37. Shao XF, Tong SC (2018) Adaptive fuzzy prescribed performance control for MIMO stochastic nonlinear systems. IEEE Access 6:76754–76767
38. Yoshimura T (2022) Prescribed performance control for MIMO stochastic discrete-time nonlinear systems in a strict-feedback form using a set of noisy measurements. Int J Syst Sci 53(4):689–703
39. Li YM, Tong SC (2015) Prescribed performance adaptive fuzzy output-feedback dynamic surface control for nonlinear large-scale systems with time delays. Information Sciences 292:125–142
40. Hua CC, Meng R, Li K, Guan XP (2020) Full state constraints-based adaptive tracking control for uncertain nonlinear stochastic systems with input saturation. J Franklin Instit 357(9):5125–5142
41. Sui S, Chen CLP, Tong SC (2021) A novel adaptive NN prescribed performance control for stochastic nonlinear systems. IEEE Trans Neural Netw Learn Syst 32(7):3196–3205
42. Liu CG, Gao C, Liu XP, Wang HQ, Zhou YC (2021) Adaptive finite-time prescribed performance control for stochastic nonlinear systems with unknown virtual control coefficients. Nonlinear Dyn 104:3655–3670
43. Liu H, Li XH, Liu XP, Wang HQ (2020) Adaptive neural network prescribed performance bounded-H_∞ tracking control for a class of stochastic nonlinear systems. IEEE Trans Neural Netw Learn Syst 31(6):2140–2152
44. Liu W, Fei SQ, Ma Q, Zhao HY, Xu SY (2022) Prescribed performance dynamic surface control for nonlinear systems subject to partial and full state constraints. Appl Math Comput 431:127318. https://doi.org/10.1016/j.amc.2022.127318
45. Zhu QD, Liu YC, Wen GX (2020) Adaptive neural network control for time-varying state constrained nonlinear stochastic systems with input saturation. Inf Sci 527:191–209
46. Wang MX, Zhu SL, Han YQ (2022) Multi-dimensional Taylor network-based control for a class of nonlinear stochastic systems with full state time-varying constraints and the finite-time output constraint. Asian J Control 24(6):3311–3325
47. Wang HQ, Chen B, Lin C (2013) Adaptive neural tracking control for a class of stochastic nonlinear systems with unknown dead-zone. Int J Innov Comput Inf Control 9(8):3257–3269
48. Bucolo M, Buscarino A, Fortuna L, Gagliano S (2021) Can noise in the feedback improve the performance of a control system? J Phys Soc Jpn 90(7):075002